Supplementary Information

Convergence of Kirkwood-Buff Integrals of Ideal and Nonideal Aqueous Solutions Using Molecular Dynamics Simulations

Jasmin Milzetti, Divya Nayar, and Nico F. A. van der Vegt*

Eduard-Zintl-Institut für Anorganische Chemie, Center of Smart Interfaces, Technische Universität Darmstadt, Alarich-Weiss-Straße 10, 64287 Darmstadt, Germany

E-Mail: vandervegt@cpc.tu-darmstadt.de

System Details

Table S1 and S2 provide a complete overview of all simulations performed. Table S3 details the charges used in all m-urea systems as compared to the original force field.

Table S1: Overview of concentrations and partial charges of simulations performed in 7 nm systems. Concentrations are given in mol l^{-1}. c_{target} denotes the target concentration and c is the concentration averaged over all NPT simulations of all systems of aqueous urea and modified urea. N_U and N_W are the number of urea and water molecules, respectively. The solute models are defined in the last column where "urea" refers to an aqueous solution of the original urea model. "U-qXX" denotes the aqueous modified urea system where the original urea partial charges are scaled down by XX %.

7 nm				
$\mathbf{c_{target}}$ $[M]$	**c** $[M]$	$\mathbf{N_U}$	$\mathbf{N_W}$	**solute**
0.5	0.486	103	11475	urea, U-q95, U-q90, U-q85, U-q80, U-q75, U-q70, U-q60, U-q50
1	0.983	207	11131	urea, U-q95, U-q90, U-q85, U-q80, U-q75, U-q70, U-q60
1.5	1.481	310	10787	urea, U-q95, U-q90, U-q85, U-q80, U-q75, U-q70, U-q60
2	1.985	413	10442	urea, U-q95, U-q90, U-q85, U-q80, U-q75, U-q70, U-q60
3	3.013	620	9754	urea, U-q95, U-q90, U-q85, U-q80, U-q75, U-q70, U-q60, U-q50
4	4.081	826	9065	urea, U-q95, U-q90, U-q85, U-q80, U-q75
5	5.159	1033	8377	urea, U-q95, U-q90, U-q85, U-q80, U-q75, U-q70, U-q60
6	6.208	1239	7800	urea, U-q95, U-q90, U-q85, U-q80, U-q75, U-q70, U-q60
7	7.229	1446	7373	urea, U-q95, U-q90, U-q85
9	8.715	1652	6311	urea, U-q95

Table S2: Overview of concentrations and partial charges of simulations performed in 4 nm systems, analogous to Table S1.

4 nm				
$\mathbf{c_{target}}$ $[M]$	**c** $[M]$	$\mathbf{N_U}$	$\mathbf{N_W}$	**solute**
1	0.981	39	2077	urea, U-q85
2	1.990	77	1948	urea, U-q85, U-q80
5	5.181	193	1563	urea, U-q85, U-q80
6	6.308	231	1435	urea, U-q85

Table S3: Partial charges used for different modified urea systems. All partial charges are given in e. The last row show the dipole moment in D. The precision of values of the partial charges is chosen such that the net charge is zero for any given model.

Atom	**urea**	**U-q95**	**U-q90**	**U-q85**	**U-q80**	**U-q75**	**U-q70**	**U-q60**	**U-q50**
C	0.921	0.87495	0.8289	0.78285	0.7368	0.69075	0.6447	0.5526	0.4605
O	-0.675	-0.64125	-0.6075	-0.57375	-0.5400	-0.50625	-0.4725	-0.4050	-0.3375
N	-0.693	-0.65835	-0.6237	-0.58905	-0.5544	-0.51975	-0.4851	-0.4158	-0.3465
H	0.285	0.27075	0.2565	0.24225	0.2280	0.21375	0.1995	0.1710	0.1425
μ	4.650	4.418	4.185	3.953	3.720	3.488	3.255	2.790	2.325

The final simulation parameters have been chosen after performing certain tests. The effect of box size and simulation length on KBI evaluation has been discussed for aqueous urea systems in the main paper. Figure S1 shows the choice of cut-off as also discussed in the main paper.

The simulation length was originally tested for the 5M urea system as shown in Figure 1 (main paper). The convergence of KBIs for lower concentrations can be improved by longer runs. Figure S2 illustrates the improvement of convergence in G_{UU} upon prolongation of the simulation for two systems where sampling is an issue; (a) moderate concentration of a nonideal aqueous urea (4 M U-q95) system and (b) low concentration of aqueous urea system (1.5 M) to (a) 90 ns and (b) 140 ns. The convergence is evaluated by examining the slope in the B-KBI, as shown in the insets. While in part (a), a clear improvement is visible, at low concentrations sufficient sampling of urea-urea pair correlations at large distances does not seem computationally affordable to obtain correct convergence behavior, as shown in part (b).

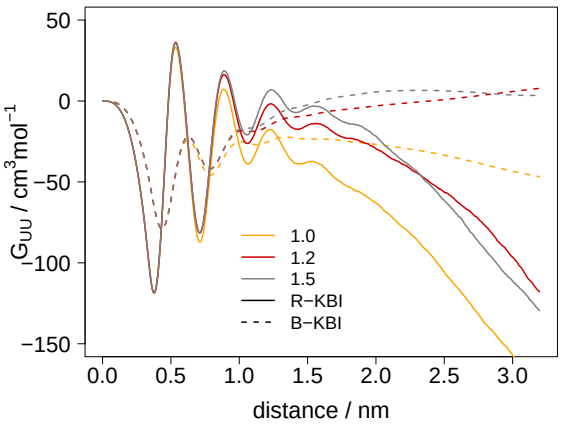

Figure S1: Influence of cut-off (in nm) on G_{UU} (R-KBI and B-KBI) for 3 M urea solutions. The box length used was 7 nm with simulation of 50 ns. The solid and dashed lines indicate the R-KBI and B-KBI respectively.

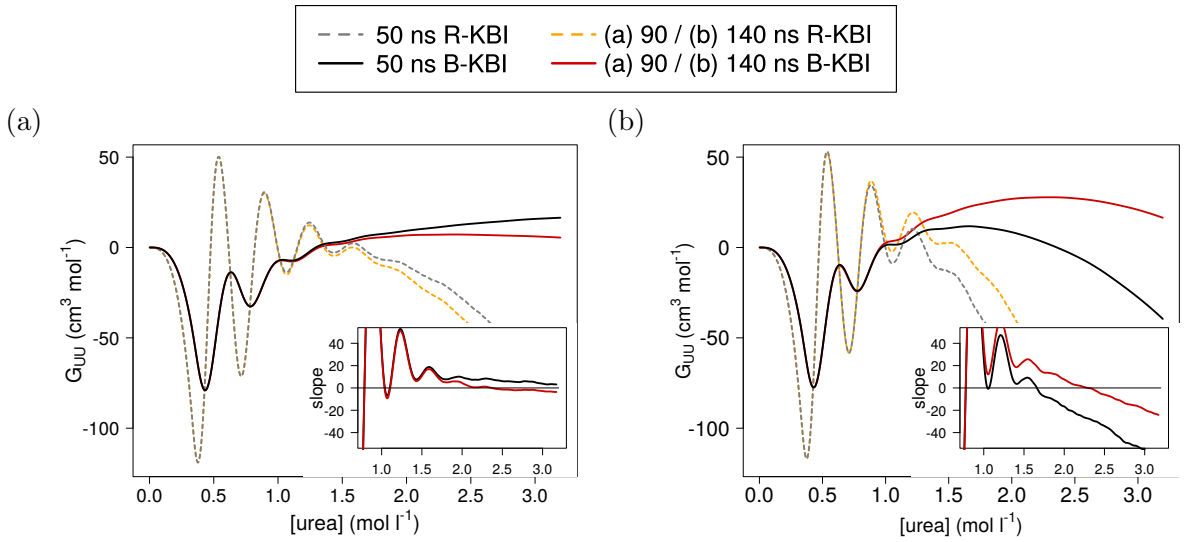

Figure S2: Improvement of KBI convergence by prolongating simulation lengths for (a) U-q95 (4 M) and (b) aqueous urea (1.5 M) systems. Insets show the slope in the tail region of R-KBI in $cm^3mol^{-1}nm^{-1}$. The slope is calculated for a secant line defined by two points of the KBI at a distance of 0.05 nm.

Computation of the Error Bars

Error bars for KBIs are calculated as the RMSD of values computed from blocks of trajectory relative to that obtained from complete trajectory. The trajectory is split into 5 blocks of length 10 ns each, from which the KBIs are calculated.

Following the central limit theorem, the error σ_A for all derived thermodynamic properties are calculated as shown in Equation 1 for a quantity A. Again, the trajectory is split into $N_{blocks} = 5$ blocks. For each block the KBIs are calculated, using which the quantity A_i is evaluated.

$$\sigma_A = \frac{1}{\sqrt{N_{blocks} - 1}} \sqrt{\frac{\sum_{i=1}^{N_{blocks}} A_i^2}{N_{blocks}} - \left(\frac{\sum_{i=1}^{N_{blocks}} A_i}{N_{blocks}} \right)^2} \tag{1}$$

Additional results

RDFs and KBIs

Figure S3 shows the RDFs for solutions of urea and U-q80 for three different concentrations each. The height of the first peak in $g_{UU}(r)$ decreases with concentration, while the peaks in $g_{UW}(r)$ and $g_{WW}(r)$ increase with concentration. These trends imply favored hydration of urea molecules with increased concentration. These trends are reflected in the KBIs, which are shown in Figure 5 and 7 (b) in the main paper. G_{UU} and G_{WW} decrease and increase, respectively. G_{UW} decreases for nonideal solutions, while it shows a non-monotonic trend for aqueous urea. Moreover, in the modified urea system multiple peaks (shells of solvation) are influenced by changes in concentration, which is not the case for aqueous urea.

Figure S4 (a) compares different RDF corrections for 2 M urea as already discussed in the main paper.

Figure S5 illustrates the performance of the Ganguly RDF correction. The magnitude of the correction Δg_{UU} increases with lower concentration (poorer sampling) and lower partial charge (more difficult sampling). The residual of the RDF to unity (σ) is sensitive to the concentration, where lower concentrations show larger deviations. This is the case because the shape of the RDF is preserved upon application of the correction, as shown in Figure S5 (a), and RDFs of lower concentrations show larger statistical noise. Consequentially, the residual can be reduced by enhanced sampling (longer trajectory) as shown for the prolonged simulation of 5 M urea. The performance of the RDF correction breaks down for U-q75, which shows traces of segregation of molecules in system.

To complement the trends in KBIs in Figure 3 and 7 (a) of the main paper, Figure S6 shows further examples of KBIs. Part (a) shows an example of a partially segregated solution which leads to non-converging KBIs and high absolute values. Part (b) is an example of poor KBI convergence due to low concentrations and can be directly compared to the urea solution in Figure 3 (a).

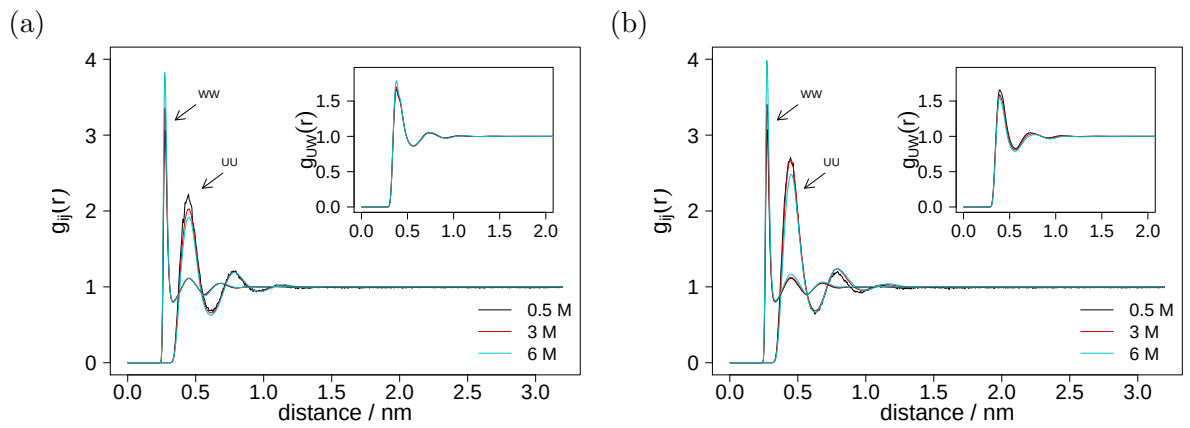

Figure S3: Radial distribution functions g_{UU}(r) and g_{WW}(r) for (a) aqueous urea and (b) U-q80 systems with varying concentrations. The inset shows g_{UW}(r) for respective systems.

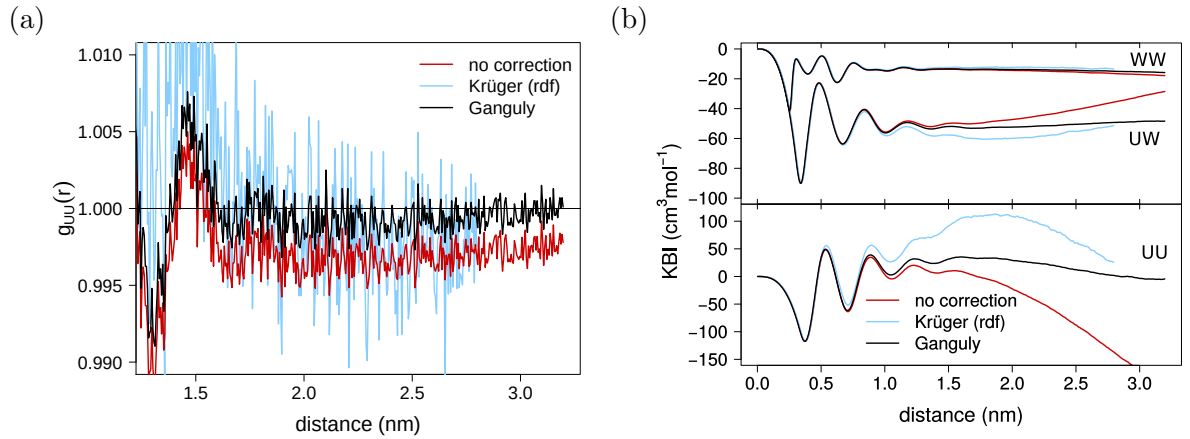

Figure S4: Comparison of RDF tail correction methods on (a) g_{UU}(r) convergence and (b) associated KBIs for 2 M urea solution (7 nm system size).

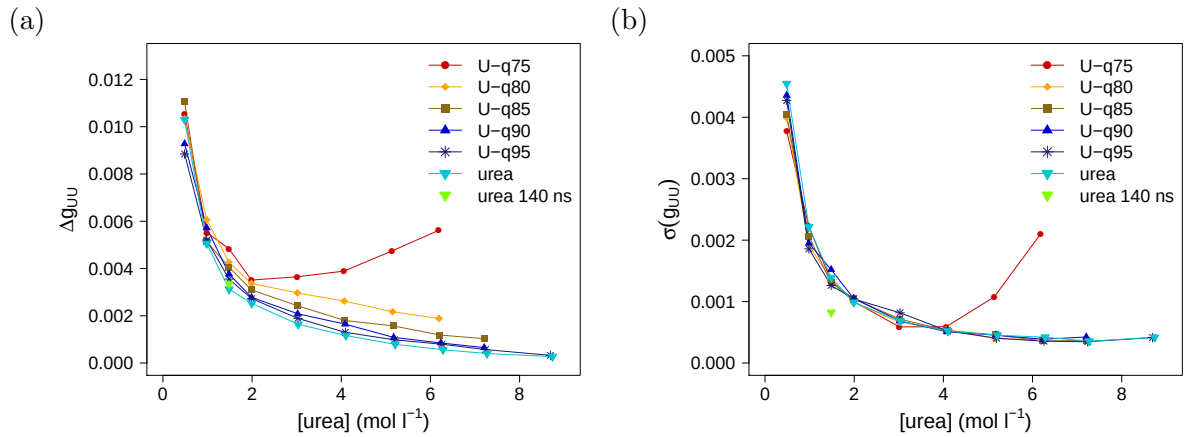

Figure S5: (a) and (b) show the performance of the Ganguly correction for all systems studied. (a) shows the average magnitude of the difference between uncorrected and corrected RDF and (b) the remaining residual (RMSD) of the RDFs from the expected value of unity. Both values are calculated in between 2.0 and 2.5 nm.

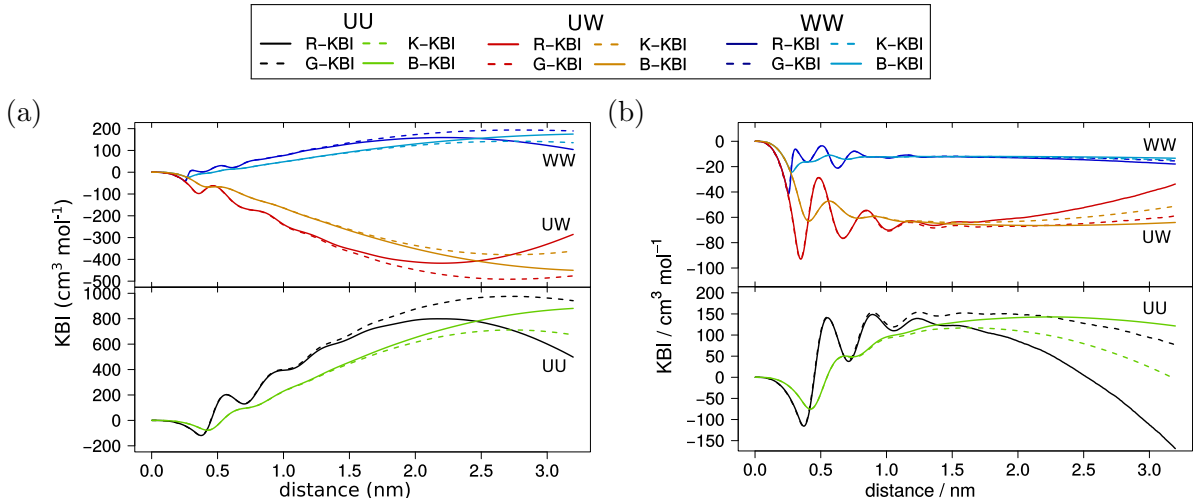

Figure S6: Comparison of convergence of KBIs, computed using different methods for nonideal (a) U-q75 (6 M) and (b) U-q85 (2 M) systems.

Thermodynamic quantities for nonideal solutions

Figure S7 (a) shows a comparison of a_{UU} values for U-q85 systems of different concentrations and methods, as has been described in the main paper.

Figure S7 (b) examines the robustness of different KBI methods for the prediction of a_{UU} for the particular case of 5 M urea. To this end, a moving average over G_{ij} is computed and each of these averaged KBIs is used to calculate the activity derivative. The CR values presented in Figure 6 (a) match exactly the value of R-KBI at 1.31 nm (orange line) whereas LR values cannot be taken directly from the figures. The data show an increased robustness of B-KBIs over R-KBIs. 4nm R-KBI is particularly sensitive to the area of averaging. Both R-KBIs show some structuring, whereas B-KBIs lead to monotonic trends at the distances investigated.

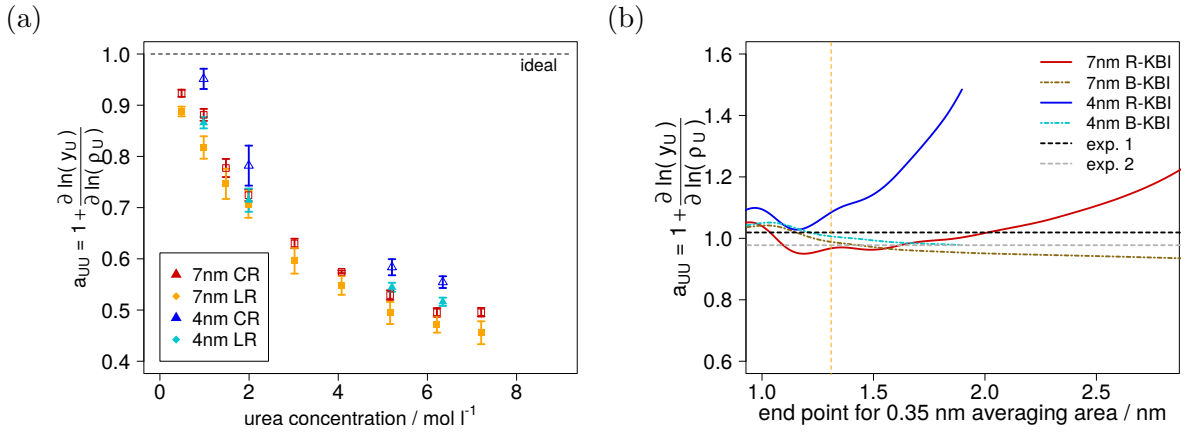

Figure S7: Urea activity coefficient derivatives a_{UU}. (a) shows different CR and LR methods for U-q85 system as a function of concentration. (b) compares the convergence behavior of different methods for 5 M urea by means of a_{UU} values obtained from different running average KBIs. Experimental data is taken from (1) Stokes[1] and (2) Miyawaki et al.,[2] as reprinted in.[3] The orange line marks R = 1.31 nm corresponding to the CR method. The corresponding final a_{UU} values can be found in Figure 6 (a) in the main paper.

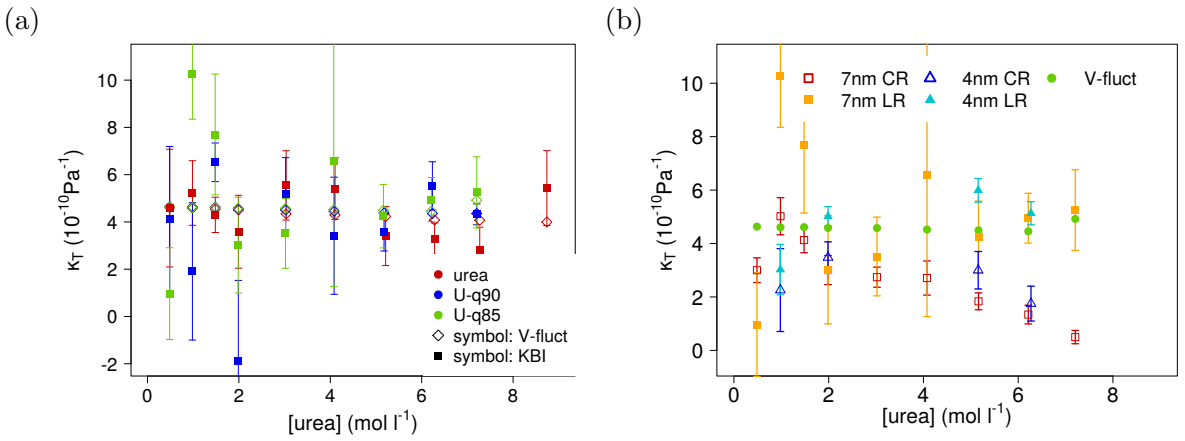

Figure S8: Isothermal compressibility, κ_T, calculated using (a) 7nm LR and volume fluctuation methods for aqueous urea, U-q90 and U-q85 systems and (b) different averaging methods for U-q85 system as a function of concentration.

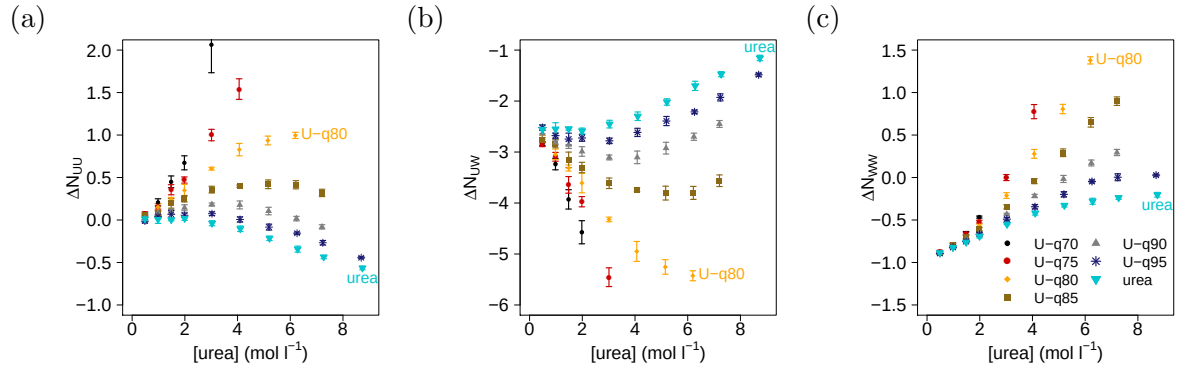

Figure S9: Excess coordination numbers, ΔN_{ij} for UU, UW and WW calculated using 7nm CR method for ideal urea-water and nonideal m-urea systems as a function of concentration.

Figure S8 (a) shows a comparison of results for different systems. It can be seen that KBI values are not accurate enough to reproduce the small changes in compressibilities stemming from the changes in ideality of the systems. Figure S8 (b) shows a comparison of different methods for the nonideal system of U-q85, as has been discussed for aqueous urea in the main paper (Figure 6 (b)).

Figure S9 shows a comparison of excess coordination numbers with varying concentration and ideality, as discussed in the main paper.

References

[1] Stokes, R. H. Thermodynamics of Aqueous Urea Solutions. *Aust. J. Chem.* **1967**, *20*, 10.

[2] Miyawaki, O.; Saito, A.; Nakamura, K. Activity and Activity Coefficient of Water in Aqueous Solutions and Their Relationships with Solution Structure Parameters. *Biosci. Biotechnol. Biochem.* **1996**, *61*, 466–469.

[3] Weerasinghe, S.; Smith, P. E. A Kirkwood - Buff Derived Force Field for Mixtures of Urea and Water. *J. Phys. Chem. B* **2003**, *107*, 3891–3898.